



OPEN ACCESS

EDITED BY
Jin Bin,
Shandong University, China

REVIEWED BY
Chaobin He,
Sun Yat-sen University Cancer Center
(SYSUCC), China
Jiangping Yang,
Kunming Medical University, China
Yaru Tian,
Shandong First Medical University and
Shandong Academy of Medical Science,
China

*CORRESPONDENCE
Chengfeng Wang
✉ drwangcf1962@163.com

†These authors have contributed
equally to this work

RECEIVED 26 March 2025
ACCEPTED 24 April 2025
PUBLISHED 15 May 2025

CITATION

Guan X, Mu Y, Jin X and Wang C (2025)
Integrated multi-omics profiling to establish
an IGFBP-based prognostic score for
pancreatic ductal adenocarcinoma:
unraveling prognostic biomarkers, immune
microenvironment crosstalk, and therapeutic
implications.
Front. Immunol. 16:1600527.
doi: 10.3389/fimmu.2025.1600527

COPYRIGHT

© 2025 Guan, Mu, Jin and Wang. This is an
open-access article distributed under the terms
of the [Creative Commons Attribution License
\(CC BY\)](#). The use, distribution or reproduction
in other forums is permitted, provided the
original author(s) and the copyright owner(s)
are credited and that the original publication
in this journal is cited, in accordance with
accepted academic practice. No use,
distribution or reproduction is permitted
which does not comply with these terms.

Integrated multi-omics profiling to establish an IGFBP-based prognostic score for pancreatic ductal adenocarcinoma: unraveling prognostic biomarkers, immune microenvironment crosstalk, and therapeutic implications

Xiao Guan[†], Yongrun Mu[†], Xin Jin[†] and Chengfeng Wang^{*}

State Key Lab of Molecular Oncology and Department of Pancreatic and Gastric Surgery, National Cancer Center/National Clinical Research Center for Cancer/Cancer Hospital, Chinese Academy of Medical Sciences and Peking Union Medical College, Beijing, China

Background: Pancreatic ductal adenocarcinoma (PDAC) is accompanied by endocrine dysfunction, particularly involving dysregulation of the insulin and insulin-like growth factor (IGF) signaling pathways. Clinical manifestations such as hyperglycemia and insulin resistance are common and have been linked to aberrant expression of insulin-like growth factor-binding proteins (IGFBPs). However, the specific roles and mechanisms of IGFBP family genes in PDAC remain unclear.

Method: We conducted a multi-dimensional integrative analysis using publicly available PDAC cohorts, stratifying patients based on IGFBP gene expression profiles. A prognostic model was constructed to classify patients into risk groups. To explore the biological mechanisms underlying IGFBP involvement in PDAC, we further incorporated single-cell transcriptomic sequencing and spatial transcriptomic data to investigate the relationship between IGFBP expression and the tumor immune microenvironment.

Result: Our prognostic model effectively stratified PDAC patients into distinct risk categories with significant survival differences. High-risk patients demonstrated specific IGFBP expression patterns associated with aggressive tumor biology. Single-cell and spatial transcriptomic analyses revealed that IGFBP family genes modulate immune cell infiltration and spatial immune heterogeneity within the tumor microenvironment.

Conclusion: This study identified the IGFBP family genes as key modulators of PDAC progression and immune landscape remodeling. These findings supported the potential of IGFBP family genes as prognostic biomarkers and therapeutic targets, offering new insights into PDAC biology and opportunities for personalized treatment strategies.

KEYWORDS

pancreatic ductal adenocarcinoma, IGFBP, prognosis, multi-omics analysis, tumor microenvironment

Introduction

Pancreatic ductal adenocarcinoma (PDAC) is one of the most lethal malignancies, characterized by a high mortality rate and rapid progression (1–4). Current projections estimate that PDAC will become the second leading cause of cancer-related deaths worldwide by 2030 (5–7). A major clinical challenge lies in the fact that most PDAC patients are diagnosed at advanced stages, often beyond the optimal window for surgical intervention, rendering curative resection infeasible (8). The disease's insidious onset, absence of early symptoms, aggressive invasiveness, and high metastatic potential significantly hinder early diagnosis and effective treatment (9). Compounding the difficulty, PDAC shows limited responsiveness to immunotherapy and inherent resistance to radiotherapy, contributing to poor clinical outcomes and dismal prognosis (10).

Currently, carcinoembryonic antigen (CEA) and carbohydrate antigen 19-9 (CA19-9) are the most commonly used clinical biomarkers for pancreatic cancer. However, their limited sensitivity and specificity, especially for early-stage disease, reduce their diagnostic utility (11). These markers often remain within normal ranges during the early phases of PDAC and only exhibit abnormal elevations at advanced disease stages (12). Thus, to improve the prognosis and overall quality of life for PDAC patients, it is imperative to investigate the molecular mechanisms underlying disease progression and to identify novel therapeutic targets and biomarkers.

The pancreas, uniquely composed of both endocrine and exocrine compartments (13, 14), exhibits anatomical and functional integration through overlapping blood supply and paracrine signaling (15, 16). Accumulating evidence suggests that interactions between these two systems may play a pivotal role in PDAC initiation and progression (17–19). For instance, in obese individuals, pancreatic β -cells have been shown to secrete cholecystokinin, which promotes tumor development (16). Conversely, PDAC cells release adrenomedullin-rich exosomes that induce β -cell apoptosis, contributing to endocrine dysfunction (20). Additionally, endocrine-disrupting compounds and hormones secreted by pancreatic endocrine cells have been implicated in the pathogenesis of PDAC (17, 21).

Among these molecular mediators, the insulin-like growth factor-binding protein (IGFBP) family has emerged as a crucial modulator. IGFBPs influence tumor growth, metastasis, and therapeutic resistance through both IGF-dependent and IGF-independent pathways, thereby contributing to PDAC progression (22, 23). These findings underscore

the biological complexity of PDAC and highlight the potential importance of the IGFBP family in tumor biology.

In this study, we conducted a comprehensive bioinformatics analysis of IGFBP family genes in PDAC. Based on IGFBP expression profiles, we established novel molecular subtypes of PDAC and stratified patients into risk-based categories. Furthermore, we integrated data from the tumor immune microenvironment, revealing immunological mechanisms potentially influenced by IGFBP activity. Taken together, our findings provide new insights into the role of IGFBPs in PDAC and lay the groundwork for developing more precise diagnostic tools and therapeutic strategies for this highly aggressive cancer.

Methods

Data collection

Gene expression profiles and clinical data for PDAC were obtained from The Cancer Genome Atlas (TCGA) and GSE62452 datasets. All non-PDAC pathological subtypes were excluded. Gene expression data were standardized, and patients lacking complete survival or clinical information were removed from the analysis. GSE202051 and GSE235315 were used for single-cell RNA sequencing and spatial transcriptomics analyses and were sourced from the Gene Expression Omnibus database.

Clustering analysis based on IGFBP family genes

Seven IGFBP family genes were selected for analysis. Patients were stratified into molecular subgroups using a consensus unsupervised clustering algorithm implemented in the “ConsensusClusterPlus” R package. We determined the optimal number of clusters using the elbow method. Clusters with high intra-group correlation and low inter-group correlation were retained for further analyses.

Multi-omics characterization of IGFBP-based subtypes

To validate the clustering results, Principal Component Analysis (PCA) was performed. Clinical characteristics were compared across subtypes, followed by Kaplan-Meier survival analysis to assess prognostic differences. The tumor microenvironment (TME) was analyzed across subtypes using various immune-related scores, and box plots were generated to visualize TME score distributions.

Differential analysis and functional enrichment

Differentially expressed genes (DEGs) between subtypes were identified. Functional enrichment analyses, including Gene Ontology (GO), Kyoto Encyclopedia of Genes and Genomes

Abbreviations: PDAC, Pancreatic ductal adenocarcinoma; IGF, insulin-like growth factor; IGFBP, IGF-binding protein; CEA, Carcinoembryonic antigen; CA19-9, Carbohydrate antigen 19-9; TCGA, The Cancer Genome Atlas; PCA, Principal Component Analysis; TME, Tumor microenvironment; DEGs, Differentially expressed genes; GO, Gene Ontology; KEGG, Kyoto Encyclopedia of Genes and Genomes; GSVA, Gene Set Variation Analysis; LASSO, Least Absolute Shrinkage and Selection Operator; TMB, Tumor mutation burden; IC50, Half-maximal inhibitory concentration; ROC, Receiver operating characteristic; DCA, Decision curve analysis; MIA, Multimodal Intersection Analysis; HR, Hazard ratio; CI, Confidence interval; mIHC, Multi-color immunohistochemistry; CM, Conditioned medium.

(KEGG), and Gene Set Variation Analysis (GSVA), were conducted to explore the biological differences among subtypes.

Clustering based on prognostic genes and risk model construction

Univariate Cox regression was applied to screen for prognostically relevant DEGs. Clustering analysis was repeated using these genes, and survival differences were reassessed. Least Absolute Shrinkage and Selection Operator (LASSO) regression was applied in the TCGA cohort to construct a prognostic model, which was validated using the GSE62452 cohort. Patients were divided into high-risk and low-risk groups based on the median risk score, and their association with IGFBP-based subtypes was evaluated.

Multi-omics analysis of the prognostic model

We assessed correlations between risk scores and clinical variables, and further analyzed TME characteristics using immune cell infiltration data. Patients were classified into immune subtypes to explore the relationship between risk score and immune phenotype. Tumor mutation burden (TMB) was calculated using somatic mutation data, and survival analyses were conducted after stratifying patients by TMB and risk score. The “pRRophetic” package was used to estimate the half-maximal inhibitory concentration (IC50) of various chemotherapeutic agents across the risk groups (24, 25).

Nomogram construction and validation

A prognostic nomogram integrating clinical variables and risk scores was developed. Calibration curves, receiver operating characteristic (ROC) curves, and decision curve analysis (DCA) were used to assess the nomogram’s predictive performance and clinical utility.

Single-cell and spatial transcriptomic analyses

For single-cell analysis, we used the Scanpy toolkit (26). Genes expressed in fewer than three cells and cells with <200 or >10,000 genes, fewer than 1000 total counts, or >20% mitochondrial/ribosomal content were excluded. SCVI (<https://github.com/scverse/scvi-tools>) was used to correct for batch effects. IGFBP gene expression levels were visualized across cell types using bar plots.

For spatial transcriptomic data, the Seurat package was used for preprocessing, including normalization, feature selection, dimensionality reduction, and clustering. Multimodal Intersection Analysis (MIA) was employed to infer cell type distributions across tissue regions. Cell types were annotated based on differentially

expressed genes in each cluster (27). CellChat was used to infer cell-cell communication networks (28).

Statistical analysis

Continuous variables were expressed as means \pm standard deviation and compared using Student’s t-test or Mann-Whitney U test. Univariate and multivariate Cox regression analyses were conducted to identify independent prognostic factors, with variables showing $P < 0.05$ in univariate analysis entered into multivariate models. Hazard ratios (HRs), 95% confidence intervals (CIs), and P-values were reported. Nomogram performance was evaluated using ROC, calibration plots, and DCA. All statistical analyses were conducted using R software (version 4.3.2), and $P < 0.05$ was considered statistically significant.

Multi-color immunohistochemistry

Briefly, 4 μ m FFEP slides was de-paraffinized in the 100% ethanol (2 \times 2min), 95% ethanol (2 \times 2min) and rinsed in distilled water, and immersed in citrate buffer after heat-induced epitope retrieval. After incubation of BSA, the AlphaTSA Multiplex IHC Kit (AXT36100031, AlphaX) was used for staining according to the manufacturer’s Guidelines. The primary antibody and the matching secondary antibody coupled with horseradish peroxidase (HRP) were incubated on the slides. Primary antibodies were IGFBP3 (Cell Signaling, Cat#64143, 1:800), CD8 (ZSGB-BIO, Cat#ZA-0508, 1:600), CD68 (Abcam, Cat#ab192847, 1:200), α -SMA (Cell Signaling, Cat#19245, 1:1200) and PANCK (Abcam, Cat#ab7753, 1:200). Fluorescent images were collected using the ZEISS Axioscan7 microscope and analyzed by ZEISS ZEN (v3.2). The Cancer Hospital Chinese Academy of Medical Science granted approval for the research.

CD8+ T cell migration assays

PANC-1 with IGFBP3-knockdown generated via siRNA (Santa cruz biotechnology, sc-39587) were cultured in DMEM supplemented with 10% fetal bovine serum under standard conditions (37°C, 5% CO₂). When cells reached 70% confluency, the culture medium was replaced with fresh serum-free DMEM. After 12 hours of incubation, the conditioned medium (CM) was collected and filtered through a 0.45 μ m sterile filter to remove cellular debris. The filtered CM was added to the lower chamber of a 24-well Transwell system (Corning Inc., pore size 8 μ m). CD8⁺ T cells were resuspended in RPMI-1640 medium at a density of 2×10^5 cells/200 μ L and seeded into the upper chamber. The plate was incubated for 24 hours under standard conditions to allow chemotactic migration toward CM-derived factors. Migrated cells on the lower membrane surface were fixed with 4% methanol-free formaldehyde (Beyotime Biotechnology) for 30 minutes at room temperature. Fixed cells were stained with 1% ammonium oxalated crystal violet (Solarbio) for 30 minutes, followed by three washes with PBS to remove excess dye.

Results

Supplementary Figure S1 showed the flowchart of this study.

Classification of PDAC into immunologically distinct subtypes based on IGFBP-based clustering analysis

A total of 309 PDAC patients from the GSE62452 and TCGA cohorts were included for further analysis. Using a consensus clustering approach based on IGFBP family gene expression, we identified two distinct molecular subtypes (Supplementary Figure S2), with the optimal number of clusters determined to be $k=2$ (Figure 1A). These subtypes were designated as Subtype A and Subtype B. PCA confirmed a clear separation between the two subtypes (Figure 1B). Kaplan–Meier survival analysis revealed that patients in Subtype A had significantly longer overall survival than those in Subtype B (Figure 1C). However, no significant differences in clinicopathological variables were observed between the subtypes (Figures 1D, E).

We next assessed immune cell infiltration characteristics between the subtypes. Subtype A exhibited a higher level of immune cell infiltration compared to Subtype B (Figure 1F). GO enrichment analysis showed that DEGs between the subtypes were mainly associated with extracellular matrix organization, membrane-bound organelles, and protein binding functions (Figure 2A). KEGG analysis indicated

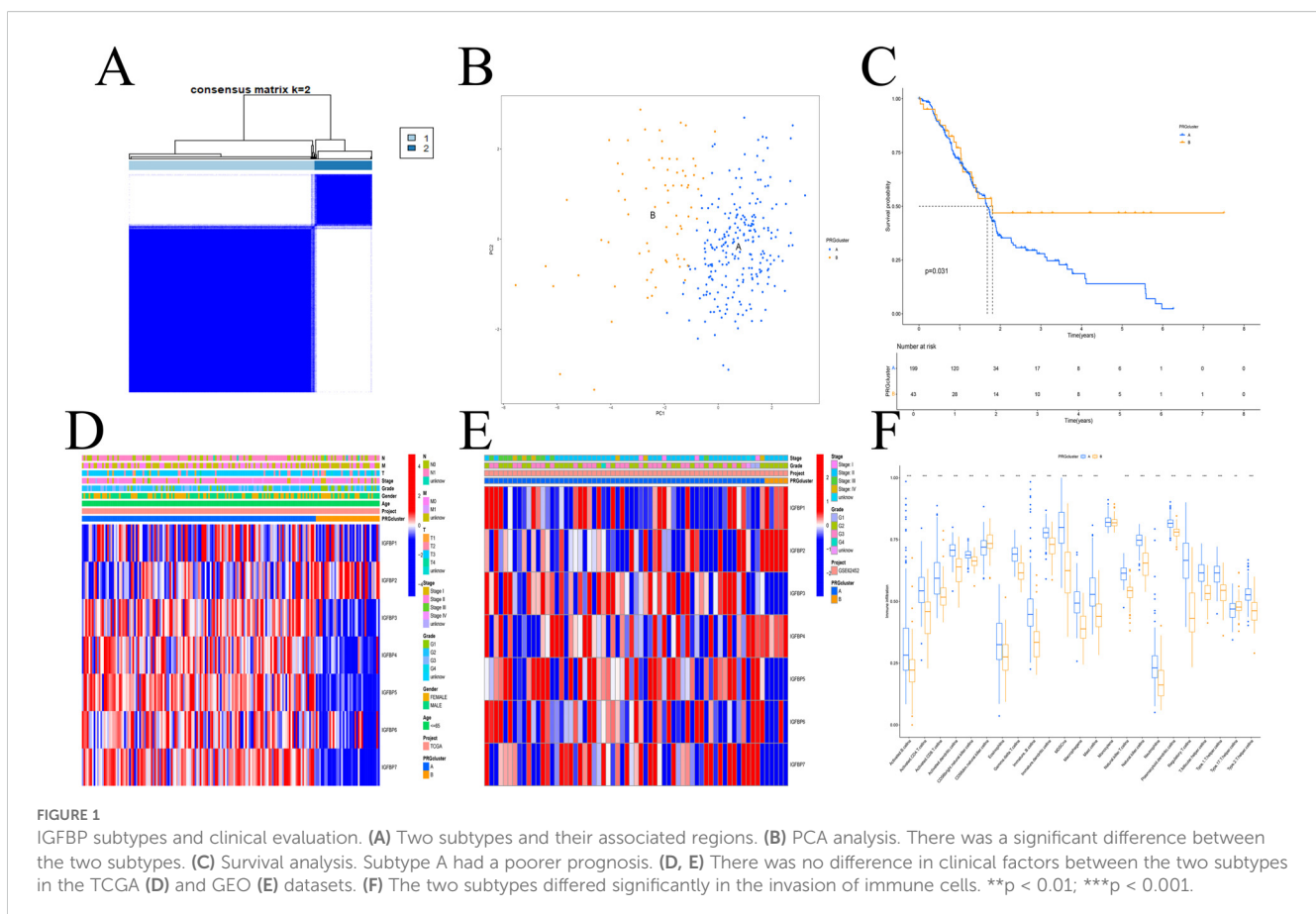
enrichment in pathways related to cell adhesion, protein processing, and ECM-receptor interactions (Figure 2B). GSVA revealed enrichment in apoptosis-related and immune signaling pathways (Figure 2C).

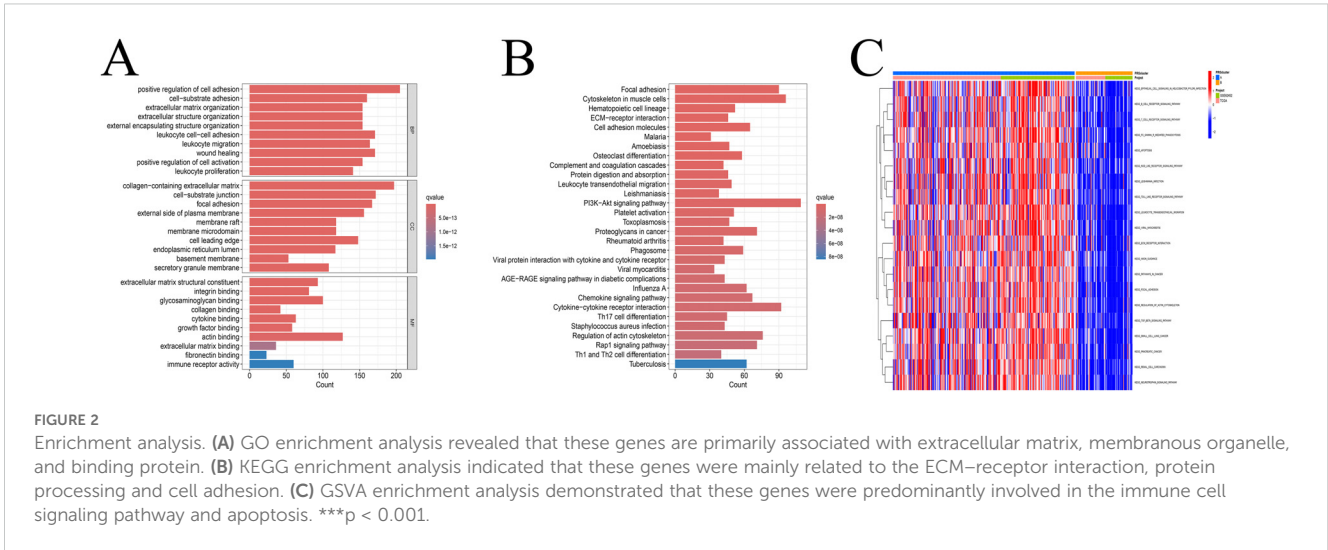
Subtype re-classification based on differentially expressed genes

Univariate and differential expression analyses identified 1303 DEGs among the IGFBP-related subtypes. Using these genes, we re-clustered the patients with the same consensus clustering method (Supplementary Figure S3), determining that three clusters ($k=3$) were optimal (Figure 3A). These new gene expression-based subtypes also showed significant survival differences (Figure 3B). Notably, the expression patterns of IGFBP family genes varied significantly among the three subtypes (Figure 3C).

Construction and evaluation of the prognostic model

Eight prognostic genes were selected using LASSO regression (Figures 4A, B). Based on the median risk score calculated from the TCGA cohort, patients were stratified into high- and low-risk groups. Figure 4C shows the distribution of patient risk scores, IGFBP subtypes, gene expression-based subtypes, and survival status. Subtype A (from





IGFBP-based clustering) was enriched in high-risk patients, while Subtype B (from gene expression-based clustering) had lower risk scores (Figures 4D, E). A positive correlation was observed between risk scores and RNAss values (Figure 4F), and IGFBP3 expression was positively associated with higher risk scores (Figure 4G).

Survival analysis demonstrated that the high-risk group had significantly worse overall survival than the low-risk group (Figure 5A). A higher proportion of deaths was observed in the high-risk group (Figure 5B). Time-dependent ROC analysis showed strong predictive accuracy of the model, with AUCs of 0.783, 0.949, and 0.922 at 1, 3, and 5 years, respectively (Figure 5D).

IGFBP-based prognostic score shows immune landscape and tumor mutational burden analysis of PDAC

Immune correlation analysis revealed that risk scores were significantly associated with the infiltration of various immune cells, including macrophages, T cells, B cells, and dendritic cells (Figure 6A,

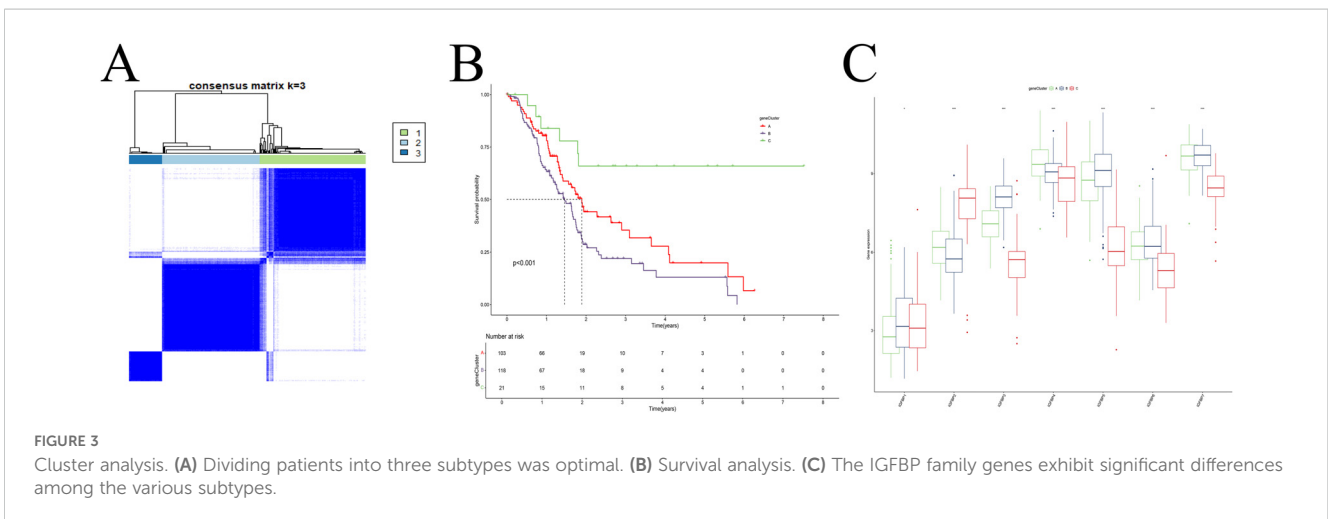
Supplementary Figure S4). Differential expression of immune checkpoint genes between the risk groups further highlighted distinct immune microenvironmental features (Figure 6B). TMB analysis identified TP53, TTN, and MUC1 as the most frequently mutated genes in both groups (Figures 6C, D). Survival analysis indicated that patients with low TMB and low-risk scores had the best prognosis (Figures 6E, F).

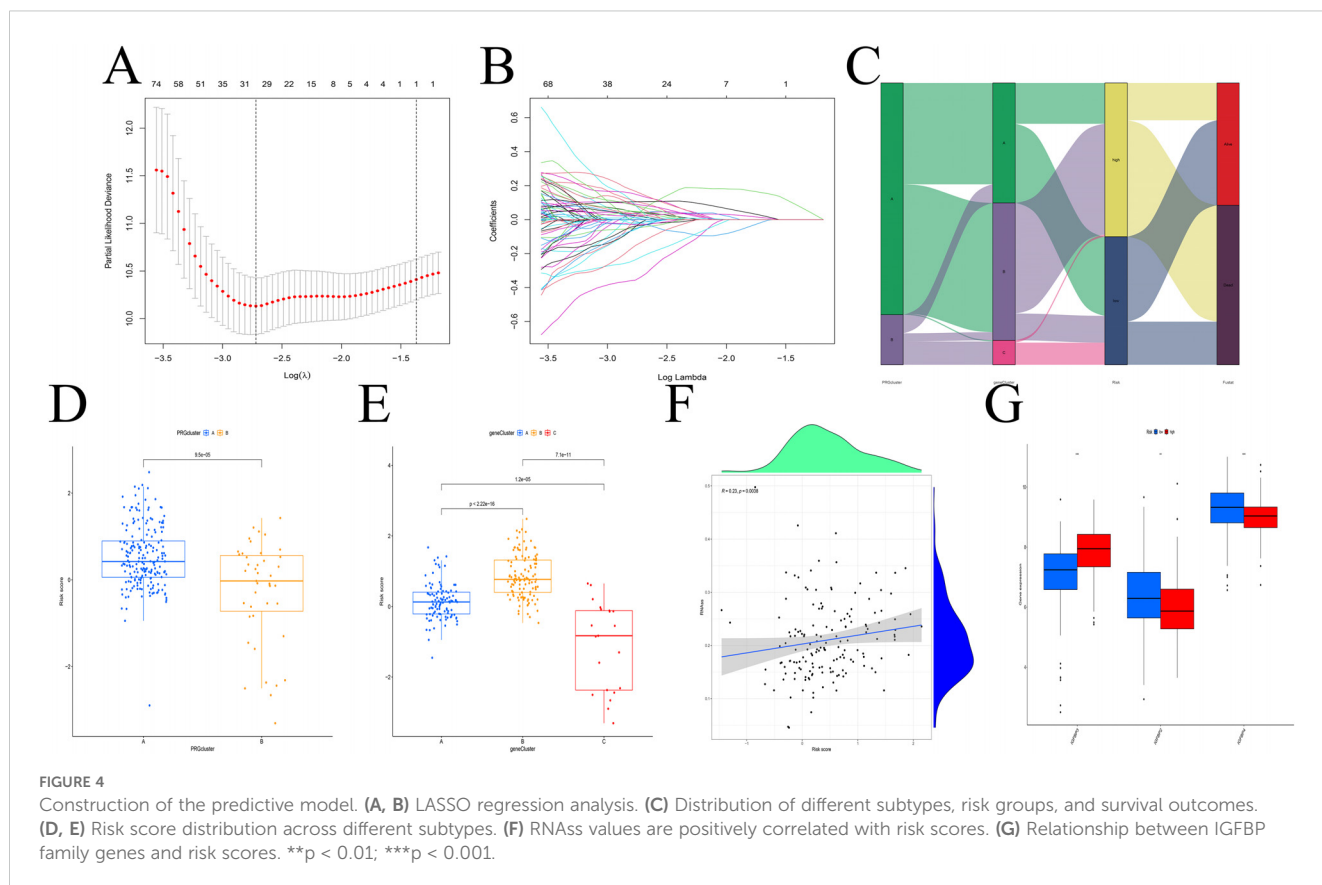
Drug sensitivity analysis

To identify potential therapeutic agents, drug sensitivity analysis was performed. High-risk patients were more sensitive to paclitaxel, epothilone B, and bleomycin (Figures 7A–C), while low-risk patients showed greater sensitivity to olaparib and veliparib (Figures 7D, E).

Nomogram development and validation

A nomogram integrating clinical variables and risk scores was constructed (Figure 8A). Calibration curves demonstrated strong





agreement between predicted and observed outcomes (Figure 8B), and decision curve analysis confirmed the clinical utility of the nomogram (Figure 8C).

Integration of single-cell and spatial transcriptomic analysis shows the spatiotemporal mapping of IGFBP family in PDAC unveils IGFBP3 hubs driving immune evasion

Using the GSE202051 dataset, we analyzed untreated single-cell RNA sequencing data. After batch normalization, malignant epithelial cells were found to express elevated levels of most IGFBP genes, except IGFBP5 and IGFBP7 (Figure 9, Supplementary Figure S5).

Following rigorous quality control, dimensionality reduction, and clustering, we identified 18 distinct cellular subpopulations within the spatial transcriptomic landscape (Figure 10A). IGFBP3 was consistently highly expressed across seven spatial samples (Figure 10B). Cell types identified in the single-cell dataset were projected onto the spatial transcriptomic data using Multimodal Intersection Analysis (MIA), allowing the localization of specific cell populations within tumor regions (Figure 10C). IGFBP3-high cells were predominantly localized in epithelial cells, primarily within the tumor core of PDAC. These IGFBP3-high regions exhibited significant enrichment of fibroblasts and B cells in their microenvironment. Cell-cell communication analysis revealed

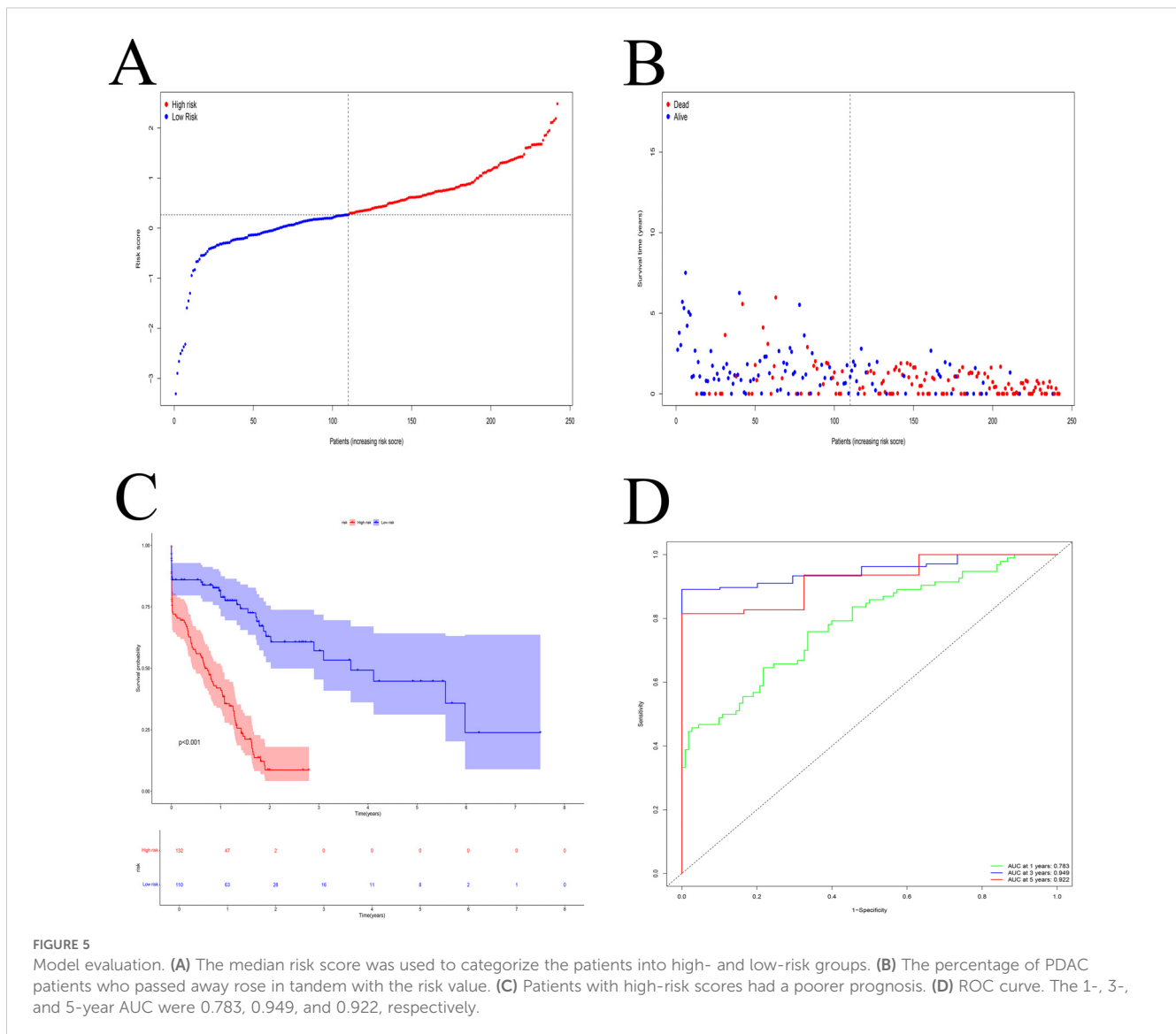
robust interactions between fibroblasts and Schwann cells via the IGF signaling axis (Figures 10D, E).

Among the IGFBP family members, IGFBP3 had the highest hazard ratio in univariate Cox regression (HR = 1.205), was highly expressed in high-risk patients, and was thus selected for further investigation.

Interestingly, we found a significant negative correlation between the risk score of the model and CD8+ T cell infiltration (Figure 6A, Supplementary Figure S4). Consistent with single-cell RNA sequencing and spatial transcriptomics data, mIHC confirmed the presence of IGFBP3 in both tumor cells and cancer-associated fibroblasts within the TME of PDAC (Figure 11). Since the spatial transcriptomics platform used in this research was the 10x Visium Cytassist version, with a resolution of 55 μ m, we conducted mIHC analysis to visually demonstrate the distance between high IGFBP3-expressing tumor cells and CD8+ T cells. Meanwhile, a higher expression of IGFBP3 indicates a worse prognosis (Supplementary Figure S6C) (HR 4.18 (95 CI 1.68-10.39)).

Furthermore, we designed a co-culture experiment, in which PANC-1 cells were co-cultured with CD8+ T cells. The results showed that after knocking down IGFBP3 in the PANC-1, the degree of CD8+ T cell infiltration significantly increased (Supplementary Figure S6D).

In terms of spatial distance, we statistically assessed the relationship between the expression of IGFBP3 in epithelial cells (PANCK) and the number of infiltrating CD8+ T cells within a 200 μ m radius (Supplementary Figures S6A, B). We found that tumor cells with high IGFBP3 expression were surrounded by significantly fewer CD8+ T cells (Supplementary Figures S6A, B). In addition, spatial



transcriptome analysis also confirmed that CD8+T cells around tumor cells with high IGFBP3 expression were significantly reduced (Supplementary Figure S7). Taken together, these findings suggest that patients with high-risk scores based on the IGFBP3-based prognostic score could be categorized as the immune exhaustion group, indicating that these high-risk patients may have limited benefit from immune therapy.

Discussion

The prognosis for pancreatic cancer remains exceedingly poor. A variety of prognostic markers have been developed, incorporating clinical parameters, laboratory indices, and molecular biomarkers (24, 29, 30). In this study, we systematically explored the role of the IGFBP family in PDAC through comprehensive bioinformatics analysis.

We first classified PDAC patients into two subtypes based on IGFBP family gene expression. Subtype A was associated with a worse prognosis. Notably, significant differences in immune cell infiltration

and immune-related functions were observed between the subtypes. We further identified three gene-based subtypes, and correlation analysis revealed that these gene signatures could reflect both patient prognosis and the characteristics of the TME. On this basis, we constructed a prognostic model using differentially expressed genes. The model's predictive performance was validated by survival analysis and ROC curves. Importantly, the risk score showed meaningful associations with TMB, immune-related signatures, clinical features, and drug sensitivity. We further developed a nomogram that integrated clinical variables and risk scores, demonstrating good performance in stratifying patients and supporting clinical decision-making.

Previous studies have highlighted the involvement of various IGFBP family members in the progression of PDAC. IGFBP1 has been found to be highly expressed in PDAC liver metastases, suggesting its potential as a clinical biomarker. Due to its role in tumor progression, IGFBP2 has also been studied extensively as a tumor biomarker (31). Xu et al. reported that plasma IGFBP2 levels in PDAC patients were significantly higher than those in patients with chronic pancreatitis, adenitis, or healthy individuals, and this elevation was

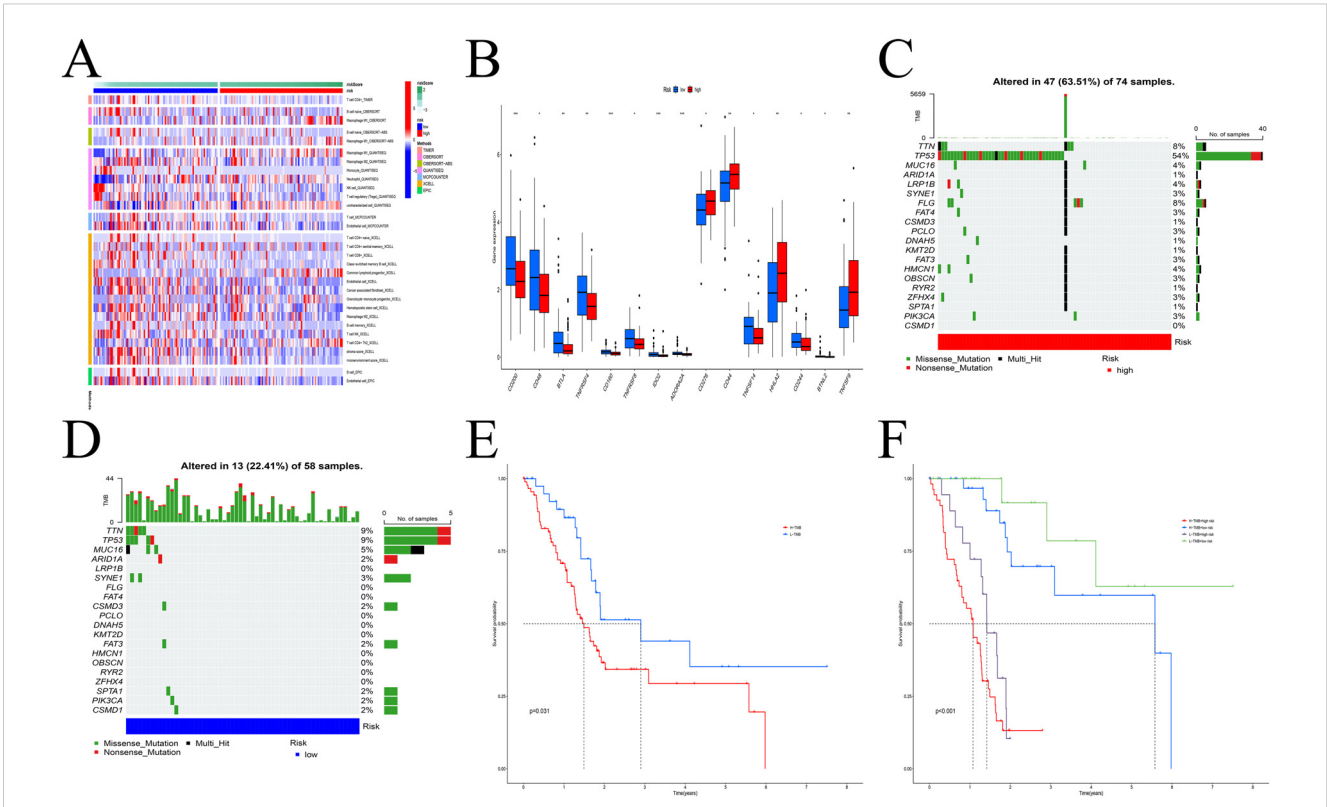


FIGURE 6 Model multi-omics analysis. **(A)** The infiltration levels of immune cells exhibited significant differences. **(B)** Variations in checkpoint gene expression levels between the two groups. **(C, D)** The frequency of gene mutations in the high **(C)** and low **(D)** risk groups. **(E, F)** Survival analysis. H-TMB had a poor prognosis. * $p < 0.05$; ** $p < 0.01$; *** $p < 0.001$.

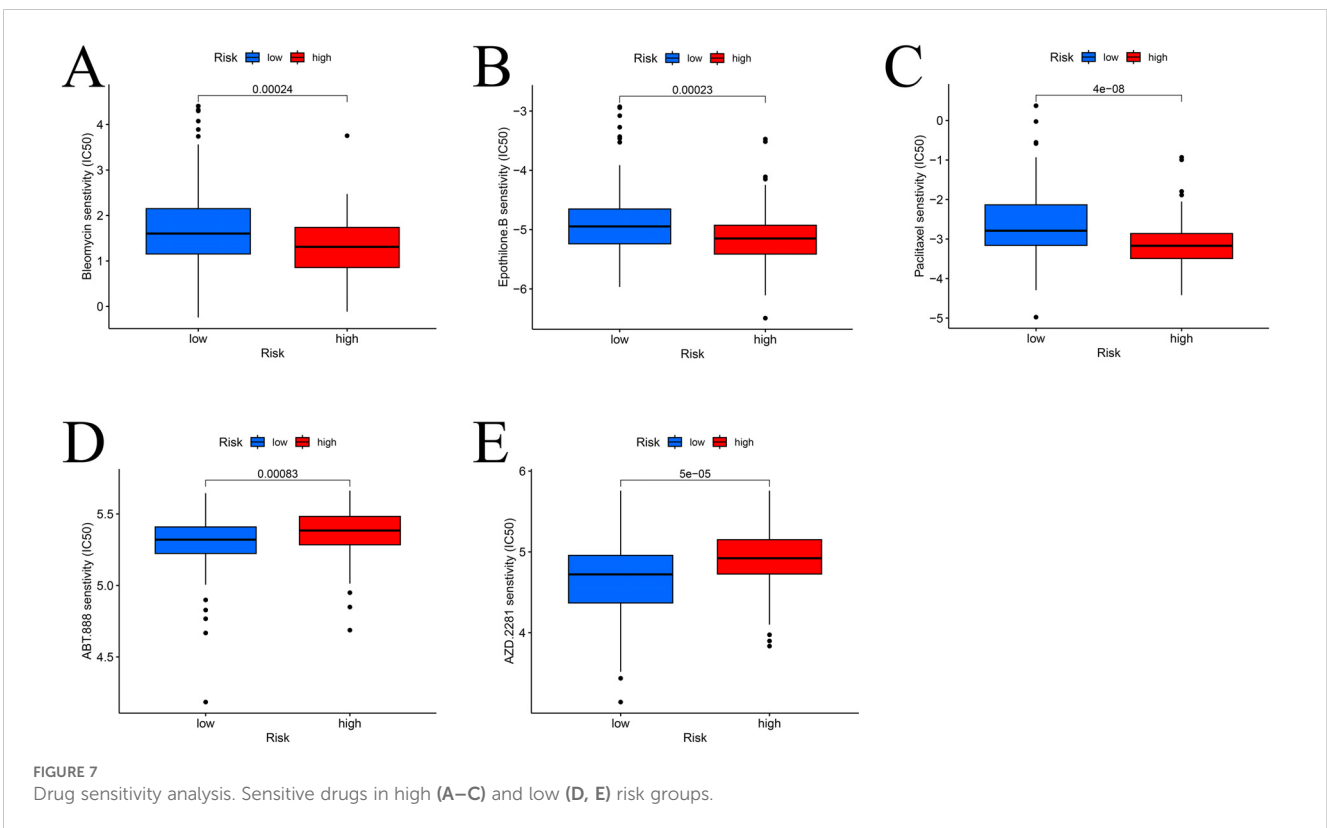
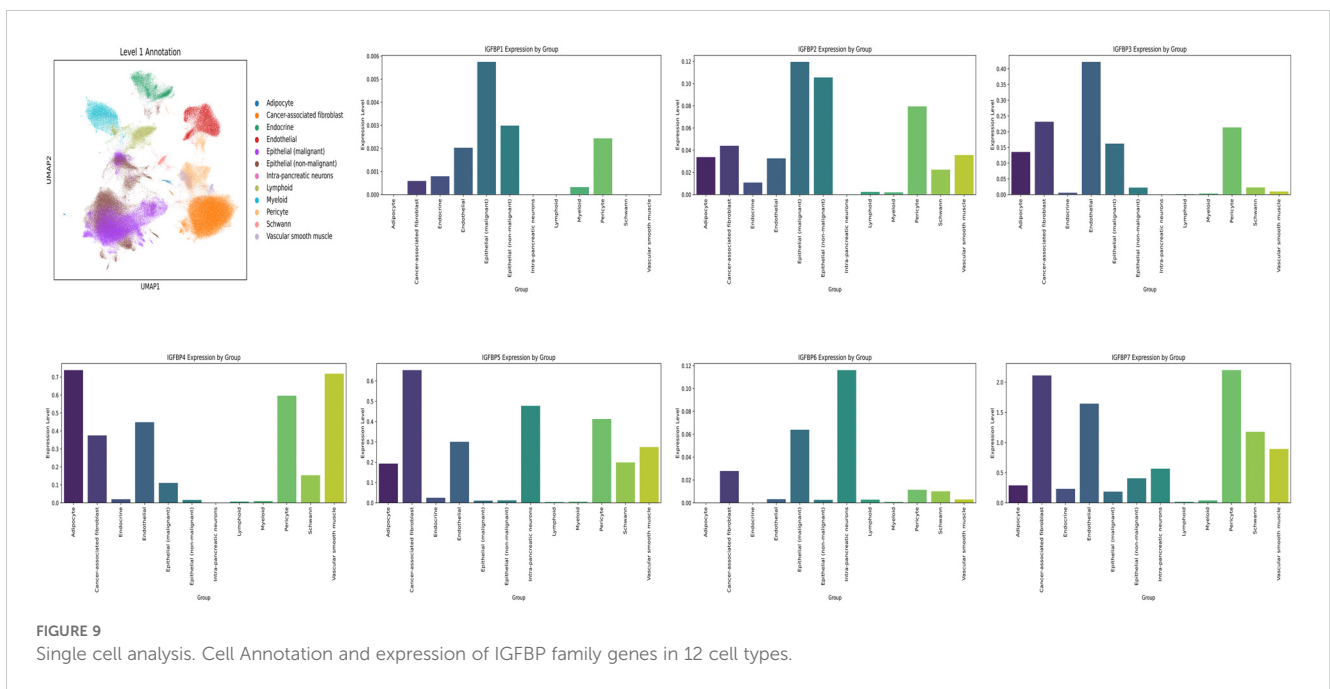
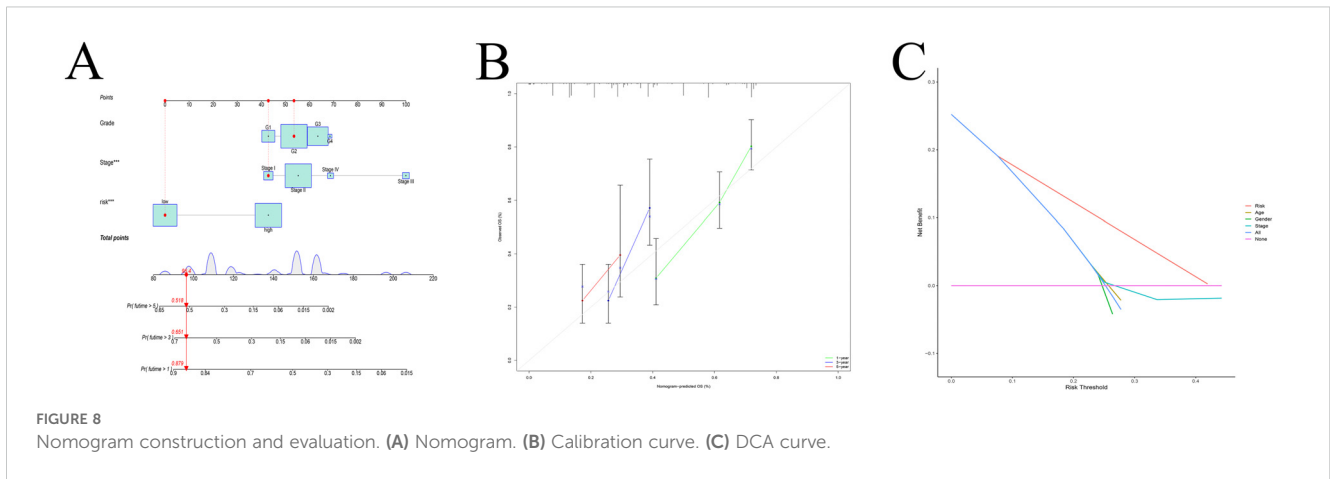


FIGURE 7 Drug sensitivity analysis. Sensitive drugs in high **(A–C)** and low **(D, E)** risk groups.

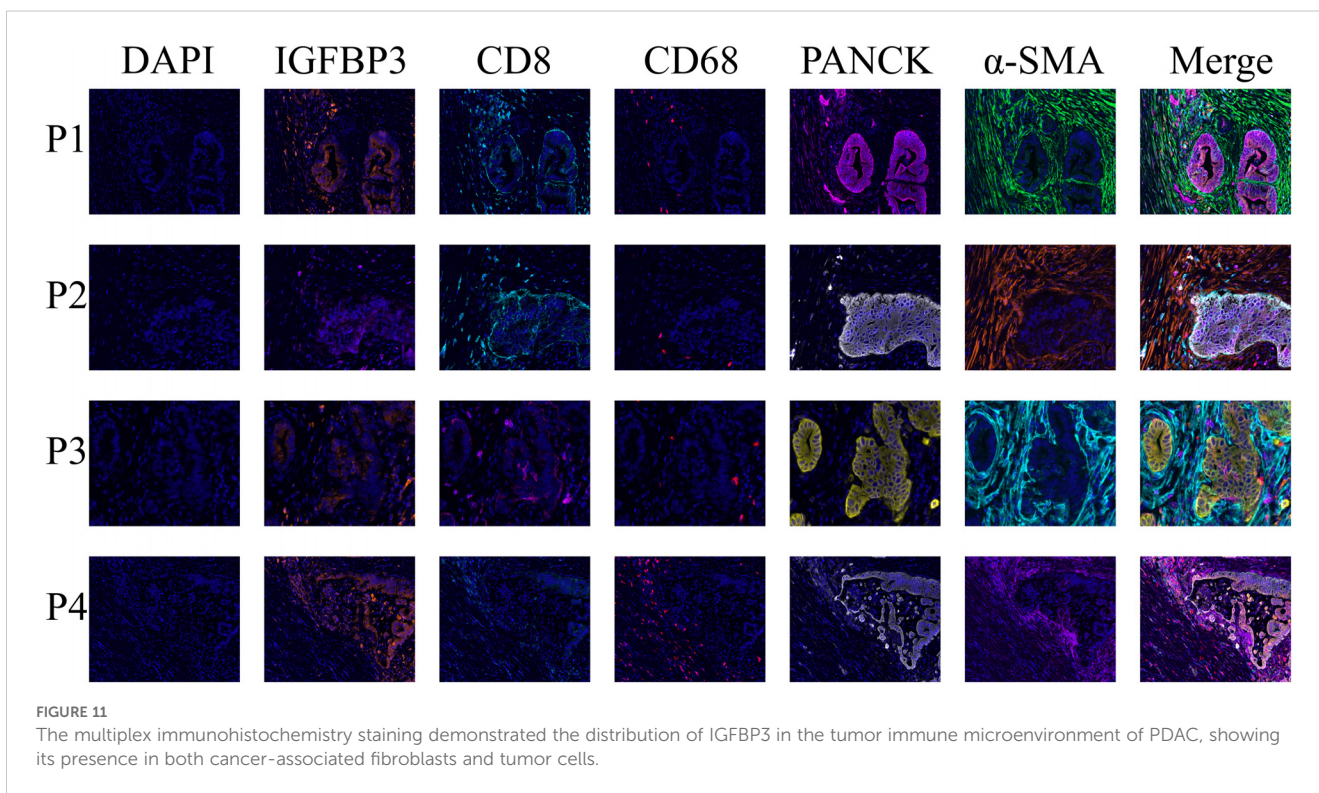
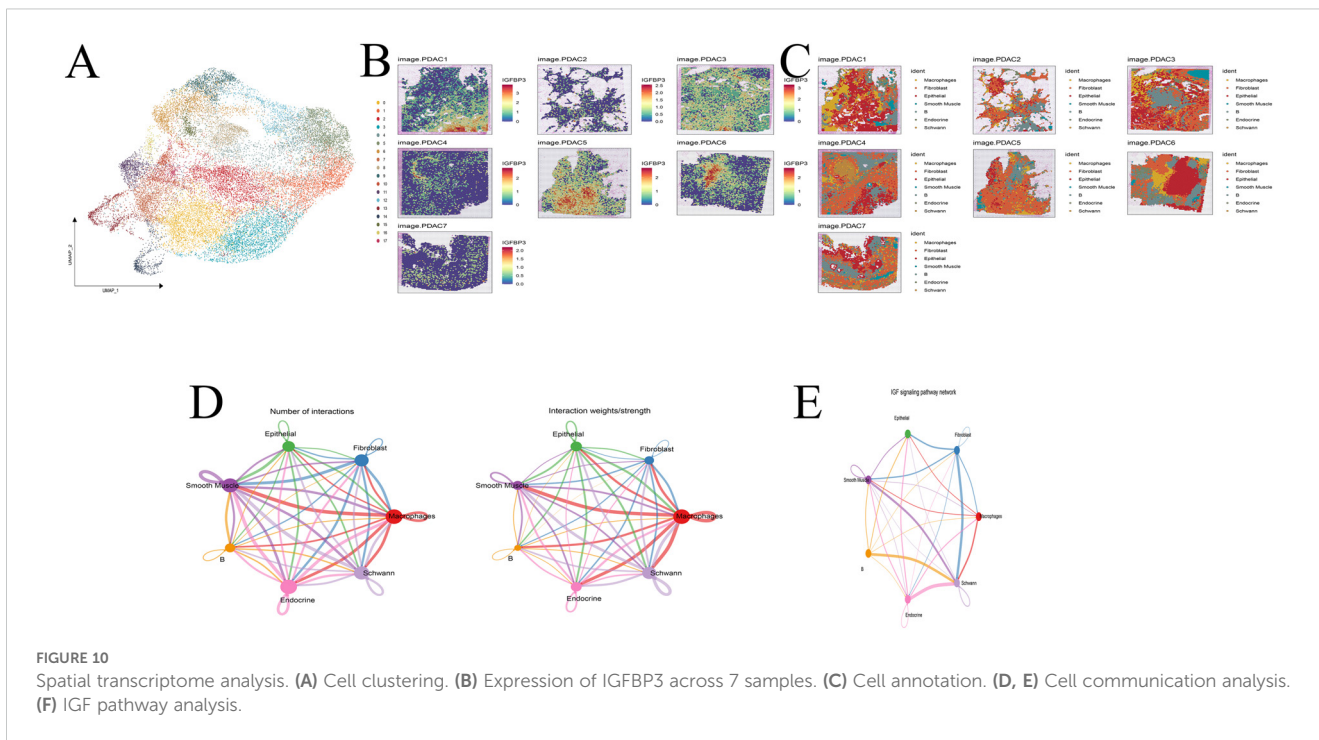


associated with poor overall survival (32). *Huang et al.* demonstrated that pancreatic cancer cells secrete IGFBP3 to induce muscle atrophy, which may contribute to cancer cachexia in patients with advanced PDAC (33). IGFBP5, a potential regulator of cell proliferation, is overexpressed in PDAC and may play a critical role in the malignant transformation of normal pancreatic epithelial cells (34). In another study, *Han et al.* found that GSG2 knockout upregulated IGFBP6 expression, thereby inhibiting the proliferation, colony formation, and migration of pancreatic cancer cells (35). IGFBP7, which is downregulated in PDAC, functions as a tumor suppressor in various cancers. Its low expression has been linked to increased cellular proliferation and poor postoperative outcomes (36). In our study, we comprehensively integrated all IGFBP family genes to develop a prognostic model, offering new insights into their collective role in PDAC progression and prognosis.

Although the IGFBP family was initially believed to function merely as passive carriers of free IGFs, emerging evidence suggests

that their biological roles extend beyond the endocrine transport of IGFs. Several IGFBPs have been reported to exhibit IGF-independent cellular functions, such as promoting cell migration without activating the IGF1 receptor (37). For instance, exogenous IGFBP3 has been shown to significantly inhibit the growth of human breast cancer cells through unique interactions with cell surface proteins (38). In pancreatic cancer, the abundant stromal compartment plays a pivotal role in regulating IGFBP expression (39). This stroma is rich in proteases capable of degrading IGFBPs, leading to elevated levels of free IGFs in the tumor microenvironment and consequently enhancing oncogenic IGF signaling (40). These biological insights underscore the rationale for incorporating IGFBP family genes into our prognostic model, aiding in the understanding of tumor biology in PDAC.

Tumor immune evasion is a well-recognized hallmark of cancer progression (41). The dynamic interaction between the immune system and tumor cells plays a crucial role in determining disease outcome (42). Factors such as tumor-infiltrating lymphocytes, TMB,



and immune checkpoint receptor expression are considered key predictors of immunotherapy efficacy (43). The PDAC TME is characterized by high immunogenicity but low immunoreactivity, marked by inadequate immune activation and pronounced immune suppression (44). Immunotolerance can arise during any stage of tumor development and is maintained or intensified via various

mechanisms, serving as a major obstacle to effective tumor immunity (45, 46). In our study, immune cell infiltration analysis revealed that immune activity was predominantly associated with the low-risk group. Furthermore, the risk score demonstrated a positive correlation with tumor purity and a negative correlation with mutational load. We also observed that several key immune

checkpoint genes were upregulated in the low-risk group, suggesting a more immunogenic profile that may benefit more from immune checkpoint blockade therapies. These findings highlight the potential of our model to guide immunotherapy strategies in PDAC patients.

In addition, TMB has been reported as a predictive marker for response to immune checkpoint inhibitors (47). Mutations in TP53, often induced by carcinogenic exposures, are independently associated with poor clinical outcomes (48). Consistent with previous reports, our analysis showed a significantly higher TP53 mutation rate in the high-risk group, further reinforcing the model's prognostic validity and its potential to inform treatment selection.

One of the long-standing challenges in PDAC treatment is drug resistance, particularly in advanced-stage disease. To address this, we investigated potential therapeutic agents based on the risk stratification provided by our prognostic model, aiming to improve drug sensitivity and treatment efficacy. Recent advances in single-cell sequencing and spatial transcriptomics have revolutionized cancer research by enabling high-resolution exploration of gene expression. In our study, we identified considerable heterogeneity in IGFBP gene expression at the single-cell level, revealing complex expression patterns within different cell populations. Spatial transcriptomics further demonstrated that IGFBP3 expression varies across tumor subregions and microenvironmental contexts, indicating its regulation by diverse cellular components.

Notably, IGFBP3 appears to be a promising therapeutic target due to its high expression in PDAC. IGFBP3 is the most abundant IGFBP in adult serum, yet its role in PDAC has not been fully elucidated. Our integrated analysis using TCGA and GEO datasets revealed that IGFBP3 exhibited the highest tumor-specific expression and prognostic relevance among all IGFBP family members. Subsequent evaluation of the tumor immune microenvironment showed that IGFBP3 is primarily expressed in tumor cells and cancer-associated fibroblasts. This finding is consistent with our single-cell sequencing data, which also revealed that IGFBP3-high tumor cells tend to be spatially distant from CD8⁺ T cells, implying potential involvement in immune evasion mechanisms.

Despite the promising findings, our study has certain limitations. The prognostic model was developed and validated using retrospective public datasets, and prospective clinical validation is needed to confirm its generalizability. Moreover, functional validation was limited to the cellular level. In future work, we aim to expand upon these findings through *in vivo* experiments and clinical studies to further substantiate the role of IGFBP3 and refine its application in PDAC management.

Conclusion

Based on the IGFBP family, we developed a robust prognostic model for PDAC and further integrated clinical parameters to construct a nomogram, which demonstrated strong predictive performance. This model enables accurate estimation of patient prognosis and characterization of TME. Moreover, the insights gained from our study may provide a foundation for novel

therapeutic strategies and contribute to the advancement of personalized treatment in PDAC.

Data availability statement

The original contributions presented in the study are included in the article/[Supplementary Material](#). Further inquiries can be directed to the corresponding author.

Ethics statement

We confirmed the study was reviewed and approved by the Cancer Hospital Chinese Academy of Medical Sciences Ethics Committee Review Board (NCC2024C-011) and all enrolled patients provided written informed consent. We confirmed that we followed to the guidelines outlined in the Declaration of Helsinki. The studies were conducted in accordance with the local legislation and institutional requirements. The participants provided their written informed consent to participate in this study.

Author contributions

YM: Writing – original draft, Writing – review & editing. XG: Writing – original draft. XJ: Writing – original draft. CW: Writing – review & editing.

Funding

The author(s) declare that financial support was received for the research and/or publication of this article. This work was supported by CAMS Innovation Fund for Medical Sciences (CIFMS, 2022-I2M-1- 010).

Acknowledgments

We were very grateful for the data provided by the TCGA and GEO databases.

Conflict of interest

The authors declare that the research was conducted in the absence of any commercial or financial relationships that could be construed as a potential conflict of interest.

Generative AI statement

The author(s) declare that no Generative AI was used in the creation of this manuscript.

Publisher's note

All claims expressed in this article are solely those of the authors and do not necessarily represent those of their affiliated organizations, or those of the publisher, the editors and the reviewers. Any product that may be evaluated in this article, or claim that may be made by its manufacturer, is not guaranteed or endorsed by the publisher.

Supplementary material

The Supplementary Material for this article can be found online at: <https://www.frontiersin.org/articles/10.3389/fimmu.2025.1600527/full#supplementary-material>

SUPPLEMENTARY FIGURE 1

The flowchart of this study.

SUPPLEMENTARY FIGURE 2

Cluster analysis. Heatmap of cellular senescence genes using cluster analysis ($k = 3-9$).

SUPPLEMENTARY FIGURE 3

Cluster analysis. Heatmap of cellular senescence genes using cluster analysis ($k = 2, 4-9$).

SUPPLEMENTARY FIGURE 4

Immunoassay of the model.

SUPPLEMENTARY FIGURE 5

Single cell analysis. IGFBP family genes expression in 12 cell types.

SUPPLEMENTARY FIGURE 6

Tumor cells with high IGFBP3 expression were surrounded by significantly fewer CD8+ T cells. A and B, mlHC analysis demonstrated that there was a relatively low level of CD8+ T cell infiltration around the IGFBP3-high epithelium. C, Kaplan-Meier survival analysis suggested that a high expression of IGFBP3 was associated with a poor prognosis. D, Knocking down IGFBP3 in the Panc1 cell line significantly increased the infiltration level of CD8+ T cells.

SUPPLEMENTARY FIGURE 7

CD8+T cells around tumor cells with high IGFBP3 expression were significantly reduced.

References

- Shi X, Zang J, Gu Q, Zhang M, Sun H, Yang L, et al. Comprehensive analysis of the multifaceted role of ITGAV in digestive system cancer progression and immune infiltration. *Front Immunol.* (2025) 16:1480771. doi: 10.3389/fimmu.2025.1480771
- Wood LD, Canto MI, Jaffee EM, Simeone DM. Pancreatic Cancer: Pathogenesis, Screening, Diagnosis, and Treatment. *Gastroenterology.* (2022) 163:386–+. doi: 10.1053/j.gastro.2022.03.056
- Siegel RL, Kratzer TB, Giaquinto AN, Sung H, Jemal A. Cancer statistics, 2025. *CA: A Cancer J Clin.* (2025) 75:10–45. doi: 10.3322/caac.21871
- Saka AH, Giaquinto AN, McCullough LE, Tossas KY, Star J, Jemal A, et al. Cancer statistics for African American and Black people, 2025. *CA: A Cancer J Clin.* (2025) 75(2):111–140. doi: 10.3322/caac.21874
- Pishvaian MJ, Blais EM, Brody JR, Lyons E, DeArbeloa P, Hendifar A, et al. Overall survival in patients with pancreatic cancer receiving matched therapies following molecular profiling: a retrospective analysis of the Know Your Tumor registry trial. *Lancet Oncol.* (2020) 21:508–18. doi: 10.1016/s1470-2045(20)30074-7
- Hu ZL, O'Reilly EM. Therapeutic developments in pancreatic cancer. *Nat Rev Gastroenterol Hepatol.* (2024) 21:7–24. doi: 10.1038/s41575-023-00840-w
- Lee YS, Lee JW, Kim HJ, Chun JW, Lee J.-C., Jang DK, et al. Survival benefits of adjuvant chemotherapy after conversion surgery in patients with advanced pancreatic cancer. *Front Oncol.* (2024) 14:1510016. doi: 10.3389/fonc.2024.1510016
- Tempero MA, Malafa MP, Al-Hawary M, Asbun H, Bain A, Behrman SW, et al. Pancreatic Adenocarcinoma, Version 2.2017, NCCN Clinical Practice Guidelines in Oncology. *J Natl Compr Canc Netw.* (2017) 15:1028–61. doi: 10.6004/jnccn.2017.0131
- Siegel RL, Miller KD, Fuchs HE, Jemal A. Cancer statistics, 2022. *CA Cancer J Clin.* (2022) 72:7–33. doi: 10.3322/caac.21708
- Hue JJ, Sugumar K, Markt SC, Hardacre JM, Ammori JB, Rothermel LD, et al. Facility volume-survival relationship in patients with early-stage pancreatic adenocarcinoma treated with neoadjuvant chemotherapy followed by pancreatoduodenectomy. *Surgery.* (2021) 170:207–14. doi: 10.1016/j.surg.2020.12.003
- Nielsen SR, Ströbech JE, Horton ER, Jackstadt R, Laitala A, Bravo MC, et al. Suppression of tumor-associated neutrophils by lorlatinib attenuates pancreatic cancer growth and improves treatment with immune checkpoint blockade. *Nat Commun.* (2021) 12:3414. doi: 10.1038/s41467-021-23731-7
- Cai J, Chen H, Lu M, Zhang Y, Lu B, You L, et al. Advances in the epidemiology of pancreatic cancer: Trends, risk factors, screening, and prognosis. *Cancer Lett.* (2021) 520:1–11. doi: 10.1016/j.canlet.2021.06.027
- Kamisawa T, Wood LD, Itoi T, Takaori K. Pancreatic cancer. *Lancet.* (2016) 388:73–85. doi: 10.1016/S0140-6736(16)00141-0
- Sheng W, Dong M, Wang G, Shi X, Gao W, Wang K, et al. The diversity between curatively resected pancreatic head and body-tail cancers based on the 8th edition of AJCC staging system: a multicenter cohort study. *BMC Cancer.* (2019) 19:981. doi: 10.1186/s12885-019-6178-z
- Rizk AA, Dybala MP, Rodriguez KC, Slak Rupnik M, Hara M. Pancreatic regional blood flow links the endocrine and exocrine diseases. *J Clin Invest.* (2023) 133(15). doi: 10.1172/jci166185
- Eibl G. Endocrine-exocrine signals in obesity-associated pancreatic cancer. *Nat Rev Gastroenterol Hepatol.* (2020) 17:455–6. doi: 10.1038/s41575-020-0324-6
- Chung KM, Singh J, Lawres L, Dorans KJ, Garcia C, Burkhardt DB, et al. Endocrine-Exocrine Signaling Drives Obesity-Associated Pancreatic Ductal Adenocarcinoma. *Cell.* (2020) 181:832–847.e818. doi: 10.1016/j.cell.2020.03.062
- Chen Y, Yin X, Xu R, Ruze R, Song J, Yin C, et al. Cancer-Associated Endocrine Cells Participate in Pancreatic Carcinogenesis. *Gastroenterology.* (2024) 167(6). doi: 10.1053/j.gastro.2024.07.016
- He P, Yang JW, Yang VW, Bialkowska AB. Krüppel-like Factor 5, Increased in Pancreatic Ductal Adenocarcinoma, Promotes Proliferation, Acinar-to-Ductal Metaplasia, Pancreatic Intraepithelial Neoplasia, and Tumor Growth in Mice. *Gastroenterology.* (2018) 154(5):1494–+. doi: 10.1053/j.gastro.2017.12.005
- Pothuraju R, Rachagani S, Junker WM, Chaudhary S, Saraswathi V, Kaur S, et al. Pancreatic cancer associated with obesity and diabetes: an alternative approach for its targeting. *J Exp Clin Cancer Res: CR.* (2018) 37:319. doi: 10.1186/s13046-018-0963-4
- Cole CL, Bachman JF, Ye J, Murphy J, Gerber SA, Beck CA, et al. Increased myocellular lipid and IGFBP-3 expression in a pre-clinical model of pancreatic cancer-related skeletal muscle wasting. *J Cachexia Sarcopenia Muscle.* (2021) 12:731–45. doi: 10.1002/jcsm.12699
- Thomas D, Radhakrishnan P. Role of Tumor and Stroma-Derived IGF/IGFBPs in Pancreatic Cancer. *Cancers (Basel).* (2020) 12(5). doi: 10.3390/cancers12051228
- Chen Y-I, Tien S-C, Ko Y-L, Chang C-C, Hsu M-F, Chien HJ, et al. SEMA7A-mediated juxtacrine stimulation of IGFBP-3 upregulates IL-17RB at pancreatic cancer invasive front. *Cancer Gene Ther.* (2024) 31:1840–55. doi: 10.1038/s41417-024-00849-6
- Zhang E, Ma Y, Liu Z, Zhang J, Liu W, Chen Y, et al. Prognostic implications and characterization of tumor-associated tertiary lymphoid structures genes in pancreatic cancer. *J Transl Med.* (2025) 23:301. doi: 10.1186/s12967-025-06152-8
- Sun S, Wang K, Guo D, Zheng H, Liu Y, Shen H, et al. Identification of the key DNA damage response genes for predicting immunotherapy and chemotherapy efficacy in lung adenocarcinoma based on bulk, single-cell RNA sequencing, and spatial transcriptomics. *Comput Biol Med.* (2024) 171:108078. doi: 10.1016/j.combiomed.2024.108078
- Wolf FA, Angerer P, Theis FJ. SCANPY: large-scale single-cell gene expression data analysis. *Genome Biol.* (2018) 19:15. doi: 10.1186/s13059-017-1382-0
- Moncada R, Barkley D, Wagner F, Chiodin M, Devlin JC, Baron M, et al. Integrating microarray-based spatial transcriptomics and single-cell RNA-seq reveals tissue architecture in pancreatic ductal adenocarcinomas. *Nat Biotechnol.* (2020) 38:333–42. doi: 10.1038/s41587-019-0392-8
- Jin S, Plikus MV, Nie Q. CellChat for systematic analysis of cell-cell communication from single-cell transcriptomics. *Nat Protoc.* (2025) 20:180–219. doi: 10.1038/s41596-024-01045-4
- Chen X, Chen Z, Guo J, Xiu Z, Chen H. Preoperative plasma fibrinogen and C-reactive protein/albumin ratio as prognostic biomarkers for pancreatic carcinoma. *Front Oncol.* (2024) 14:1301059. doi: 10.3389/fonc.2024.1301059
- Döring C, Peer K, Bankov K, Bollmann C, Ramaswamy A, Di Fazio P, et al. Whole-exome sequencing of calcitonin-producing pancreatic neuroendocrine

neoplasms indicates a unique molecular signature. *Front Oncol.* (2023) 13:1160921. doi: 10.3389/fonc.2023.1160921

31. Thakur A, Bollig A, Wu J, Liao DJ. Gene expression profiles in primary pancreatic tumors and metastatic lesions of Ela-c-myc transgenic mice. *Mol Cancer.* (2008) 7:11. doi: 10.1186/1476-4598-7-11
32. Xu J, Song Y, Zhou B, Yuan S, Gao S. Prognostic and diagnostic value of circulating IGFBP2 in pancreatic cancer. *Open Med (Wars).* (2024) 19:20230893. doi: 10.1515/med-2023-0893
33. Huang XY, Huang ZL, Yang JH, Xu YH, Sun JS, Zheng Q, et al. Pancreatic cancer cell-derived IGFBP-3 contributes to muscle wasting. *J Exp Clin Cancer Res.* (2016) 35:46. doi: 10.1186/s13046-016-0317-z
34. Sun Y, Weng X, Chen W, Ge J, Ding B, Ru J, et al. MYBBP1A-mediated IGFBP4 promoter methylation promotes epithelial-mesenchymal transition and metastasis through activation of NOTCH pathway in liver cancer. *Int J Oncol.* (2025) 66(1). doi: 10.3892/ijo.2024.5710
35. Han X, Kuang T, Ren Y, Lu Z, Liao Q, Chen W, et al. Haspin knockdown can inhibit progression and development of pancreatic cancer *in vitro* and *in vivo*. *Exp Cell Res.* (2019) 385:111605. doi: 10.1016/j.yexcr.2019.111605
36. An W, Ben QW, Chen HT, Zheng JM, Huang L, Li GX, et al. Low expression of IGFBP7 is associated with poor outcome of pancreatic ductal adenocarcinoma. *Ann Surg Oncol.* (2012) 19:3971-8. doi: 10.1245/s10434-012-2407-2
37. Lin YW, Weng XF, Huang BL, Guo HP, Xu YW, Peng YH, et al. IGFBP-1 in cancer: expression, molecular mechanisms, and potential clinical implications. *Am J Transl Res.* (2021) 13:813-32.
38. Brosseau C, Pirianov G, Colston KW. Role of insulin-like growth factor binding protein-3 in 1, 25-dihydroxyvitamin-d 3 -induced breast cancer cell apoptosis. *Int J Cell Biol.* (2013) 2013:960378. doi: 10.1155/2013/960378
39. Weniger M, Honselmann KC, Liss AS. The Extracellular Matrix and Pancreatic Cancer: A Complex Relationship. *Cancers (Basel).* (2018) 10(9). doi: 10.3390/cancers10090316
40. Jakubowska K, Pryczynicz A, Januszewska J, Sidorkiewicz I, Kemona A, Niewiński A, et al. Expressions of Matrix Metalloproteinases 2, 7, and 9 in Carcinogenesis of Pancreatic Ductal Adenocarcinoma. *Dis Markers.* (2016) 2016:9895721. doi: 10.1155/2016/9895721
41. Batlle E, Massagué J. Transforming Growth Factor- β Signaling in Immunity and Cancer. *Immunity.* (2019) 50:924-40. doi: 10.1016/j.immuni.2019.03.024
42. Gajewski TF, Schreiber H, Fu YX. Innate and adaptive immune cells in the tumor microenvironment. *Nat Immunol.* (2013) 14:1014-22. doi: 10.1038/ni.2703
43. Bear AS, Vonderheide RH, O'Hara MH. Challenges and Opportunities for Pancreatic Cancer Immunotherapy. *Cancer Cell.* (2020) 38:788-802. doi: 10.1016/j.ccell.2020.08.004
44. Werba G, Weissinger D, Kawaler EA, Zhao E, Kalfakakou D, Dhara S, et al. Single-cell RNA sequencing reveals the effects of chemotherapy on human pancreatic adenocarcinoma and its tumor microenvironment. *Nat Commun.* (2023) 14:797. doi: 10.1038/s41467-023-36296-4
45. Jain T, Dudeja V. The war against pancreatic cancer in 2020 - advances on all fronts. *Nat Rev Gastroenterol Hepatol.* (2021) 18:99-100. doi: 10.1038/s41575-020-00410-4
46. Ho WJ, Jaffee EM, Zheng L. The tumour microenvironment in pancreatic cancer - clinical challenges and opportunities. *Nat Rev Clin Oncol.* (2020) 17:527-40. doi: 10.1038/s41571-020-0363-5
47. Marabelle A, Fakih M, Lopez J, Shah M, Shapira-Frommer R, Nakagawa K, et al. Association of tumour mutational burden with outcomes in patients with advanced solid tumours treated with pembrolizumab: prospective biomarker analysis of the multicohort, open-label, phase 2 KEYNOTE-158 study. *Lancet Oncol.* (2020) 21:1353-65. doi: 10.1016/s1470-2045(20)30445-9
48. Casalini R, Romei C, Ciampi R, Ramone T, Prete A, Gambale C, et al. Minor role of TP53 and TERT promoter mutations in medullary thyroid carcinoma: report of new cases and revision of the literature. *Endocrine.* (2025) 87:243-51. doi: 10.1007/s12020-024-03990-2